

Neural stem cells display an inherent mechanism for rescuing dysfunctional neurons

Jitka Ourednik^{1,2,5*†}, Václav Ourednik^{1,2,5†}, William P. Lynch³, Melitta Schachner^{1,4‡}, and Evan Y. Snyder^{2*†}

Published online 15 October 2002; doi:10.1038/nbt750

We investigated the hypothesis that neural stem cells (NSCs) possess an intrinsic capacity to “rescue” dysfunctional neurons in the brains of aged mice. The study focused on a neuronal cell type with stereotypical projections that is commonly compromised in the aged brain—the dopaminergic (DA) neuron. Unilateral implantation of murine NSCs into the midbrains of aged mice, in which the presence of stably impaired but nonapoptotic DA neurons was increased by treatment with 1-methyl-4-phenyl-1,2,3,6-tetrahydropyridine (MPTP), was associated with bilateral reconstitution of the mesostriatal system. Functional assays paralleled the spatiotemporal recovery of tyrosine hydroxylase (TH) and dopamine transporter (DAT) activity, which, in turn, mirrored the spatiotemporal distribution of donor-derived cells. Although spontaneous conversion of donor NSCs to TH⁺ cells contributed to nigral reconstitution in DA-depleted areas, the majority of DA neurons in the mesostriatal system were “rescued” host cells. Undifferentiated donor progenitors spontaneously expressing neuroprotective substances provided a plausible molecular basis for this finding. These observations suggest that host structures may benefit not only from NSC-derived replacement of lost neurons but also from the “chaperone” effect of some NSC-derived progeny.

The therapeutic potential of neural stem cells (NSCs) for CNS diseases derives in part from the fact that these cells, after transplantation, are attracted to neurodegenerative environments, where they seem to replace dead or dysfunctional cells^{1–5}. Moreover, if genetically engineered *ex vivo* to overexpress specific therapeutic molecules, they are capable of delivering those substances effectively to the desired targets⁶. Although such behaviors have been observed in the CNS undergoing acute cell death, it remains unclear whether NSCs can influence more protracted disintegration of cellular function, in which cell death is only a terminal end-stage event (e.g., during aging). In the present work, we focused on a well-characterized neuronal cell type that is gradually compromised in the aged brain—the dopaminergic (DA) neuron.

To obtain a defined, experimentally accessible population of permanently impaired (but nonnecrotic, nonapoptotic) DA neurons, we chose MPTP for its faithful replication and acceleration of neurodegenerative phenomena accompanying idiopathic Parkinson’s disease⁷. Repetitive systemic treatment of aged mice⁸ caused fiber degeneration in the basal forebrain followed by dysfunction of mesostriatal DA neurons, characterized by lifelong loss of tyrosine hydroxylase (TH) activity (the rate-limiting enzyme in DA synthesis)^{9–12}. In view of the findings from our earlier studies with primary fetal neocortical grafts^{13,14}, we then asked what effect implanted NSCs might have in aged brain containing a large population of dysfunctional but living neural cells in various stages of dissolution. We found not only that such cells could integrate widely within even the aged brain and effect a degree of cell replacement, but, importantly, that host cell rescue—as an intrinsic action of NSCs—was an unexpected major force in tissue recovery, altering the host environment such that the function of imperiled endogenous neurons was reactivated or preserved.

Results

A model of selective neuronal impairment without cell death. Aged mice received repeated injections of high-dose MPTP^{8,15,16}, creating selective metabolic stress and permanent downregulation of TH function (without cell death) in DA neurons of the mesostriatal nuclei. To validate this model, we examined brains of lesioned mice at various intervals following MPTP injection (Supplementary Fig. 1 online). The total number of neurons (neuronal nuclear antigen–positive (NeuN⁺) cells) that also expressed TH within the mesostriatal nuclei (i.e., substantia nigra (SN) pars compacta and pars lateralis, and ventral tegmental area (VTA)) was compared with that from age-matched, noninjected controls (Fig. 1). By one week post-MPTP, the number of TH⁺ cells in SN/VTA decreased bilaterally by $61 \pm 5\%$ (Fig. 1A,B) and persisted in all animals for at least the seven-week experimental time course (but remained diminished in these aged animals throughout their lives). This was paralleled by a reduction in TH immunoreactivity in both striata (Fig. 3C,D), the projection targets for mesostriatal DA neurons. The total number of NeuN⁺ cells in SN/VTA of MPTP-treated mice, however, did not differ from age-matched intact controls and remained undiminished (Fig. 1C, D); the same number of SN/VTA neurons were present pre- and post-MPTP. Thus, downregulation of TH in the mesostriatal system was achieved without death of DA neurons. Because the defect was bilateral, the typical amphetamine-induced rotation from DA asymmetry (as seen following unilateral lesioning with 6-hydroxydopamine) was appropriately not seen. Motor deficits and tremor—typical only of certain MPTP-treated primate species—were neither observed nor expected^{10,17}.

Unilateral implantation of NSCs for a bilateral disease. Cells from the *lacZ*-expressing murine NSC clone C17.2 (refs 18–22) were

¹Department of Neurobiology, Swiss Federal Institute of Technology, Hoenggerberg, CH-8093, Switzerland. ²Department of Neurology, Harvard Medical School, Harvard Institutes of Medicine, Boston, MA 02115, USA. ³Department of Microbiology/Immunology, Northeastern Ohio Universities College of Medicine, Rootstown, OH 44272, USA. ⁴Center for Molecular Neurobiology Hamburg, University of Hamburg, Martinistrasse 52, 20246 Hamburg, Germany. ⁵Department of Biomedical Sciences, College of Veterinary Medicine, Iowa State University, Ames, IA 50011, USA. *Corresponding authors (esnyder1@caregroup.harvard.edu; joured@iastate.edu.). †These authors contributed equally to this work. ‡These authors, ordered alphabetically, contributed equally to this work.

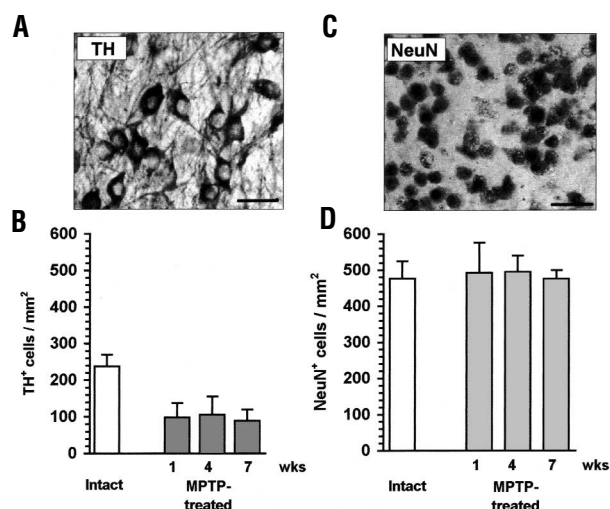


Figure 1. Effect of MPTP treatment on TH expression and the total number of neurons in SN (pars compacta and lateralis) and VTA in nongrafted mice. The total number of neurons (NeuN⁺ cells) in the mesencephalon of aged MPTP-lesioned mice remained unchanged while the percentage of TH⁺ cells decreased substantially, suggesting a stable inactivation of most TH-expressing neurons in the mesostriatal system. The numbers of cells per mm² of TH⁺ (visualized in (A) and quantified in (B)) and NeuN⁺ (visualized in (C) and quantified in (D)) cells were compared between the intact (white columns) and the MPTP-lesioned (gray columns) animals at one, four, and seven weeks post MPTP exposure. Whereas the number of TH⁺ cells decreased substantially (~60%) within the first week in animals exposed to the neurotoxin and remained low throughout the following six weeks (and lifelong in animals allowed to live out their lifespan), the number of NeuN⁺ cells remained constant in both groups. Bars, 20 μ m.

implanted unilaterally above the right SN/VTA (Fig. 2C) either one or four weeks following MPTP intoxication (Supplementary Fig. 1 online). Interestingly, three days after NSC transplantation, several of the NSC-grafted MPTP-treated animals started to rotate spontaneously contralaterally to the site of implantation, suggesting an asymmetry in DA activity. For confirmation, animals were injected with D-amphetamine, an indirect agonist stimulating DA release²³ (Fig. 2A,B). Although D-amphetamine injected into control mice (intact and mock-grafted) failed to evoke rotational behavior, it stimulated rotation in all transplanted, MPTP-treated animals (typically >20 turns/min) (Fig. 2A,B solid lines). This evidence of asymmetric function coincided with histological evidence of unilateral re-expression of TH activity in SN/VTA and their striatal projections ipsilateral to the NSC implantation (Fig. 3E, F). However, the DA imbalance diminished progressively with time and disappeared completely by the end of the second week post-transplantation (Fig. 2A, B), again consistent with the evolving pattern of TH re-expression, which was now bilateral (Fig. 3G, H), mirrored by the migration of donor-derived cells to the contralateral side (Fig. 2D–F). Neither spontaneous recovery of TH function nor changes in motor behavior were ever observed in mock-grafted MPTP-treated animals, three weeks (Fig. 3C, D) or even seven weeks after drug administration. Cells from nonneural tissues (fetal liver or heart) did not replicate this effect, suggesting the specificity of this graft-dependent recovery.

Tracking donor cells. Donor NSCs were detected by immunohistochemical staining for *Escherichia coli* β -galactosidase (β -gal). While β -gal⁺ cells were present in all grafted brains, their distribution was more extensive throughout the parenchyma and much further from the injection tract in brains of MPTP-lesioned mice (Fig. 2D and F, parts c–f) than in brains of intact mice (Fig. 2D and E,

parts a, b) and, interestingly, was also more widespread in intact aged (Fig. 2E, part b) than in intact young mice (Fig. 2E, part a). In all cases, by one week after transplantation into the damaged host brains (Fig. 2F, parts c, d), grafted NSCs were distributed principally on the ipsilateral side of the mesencephalon, consistent with the rotational behavior described above. However, by three weeks (Fig. 2F, parts e, f), they were found in high density on the contralateral side as well (also consistent with the loss of rotational behavior), and were also present in other brain regions, with some NSC progeny reaching as far as the hippocampus and neocortex. Surprisingly, the majority (~80–90%) of the β -gal⁺ cells were located not within the mesostriatal nuclei but rather surrounding the impaired DA neurons (Fig. 2F, parts c–f). These findings suggested that the extensive migration by NSCs previously reported in developing^{5,20}, immature²², and injured adult^{2,18} brains pertained as well to the aged brain, particularly when pathology was present. These observations begged for further characterization of the role of donor NSCs in the grafted animals.

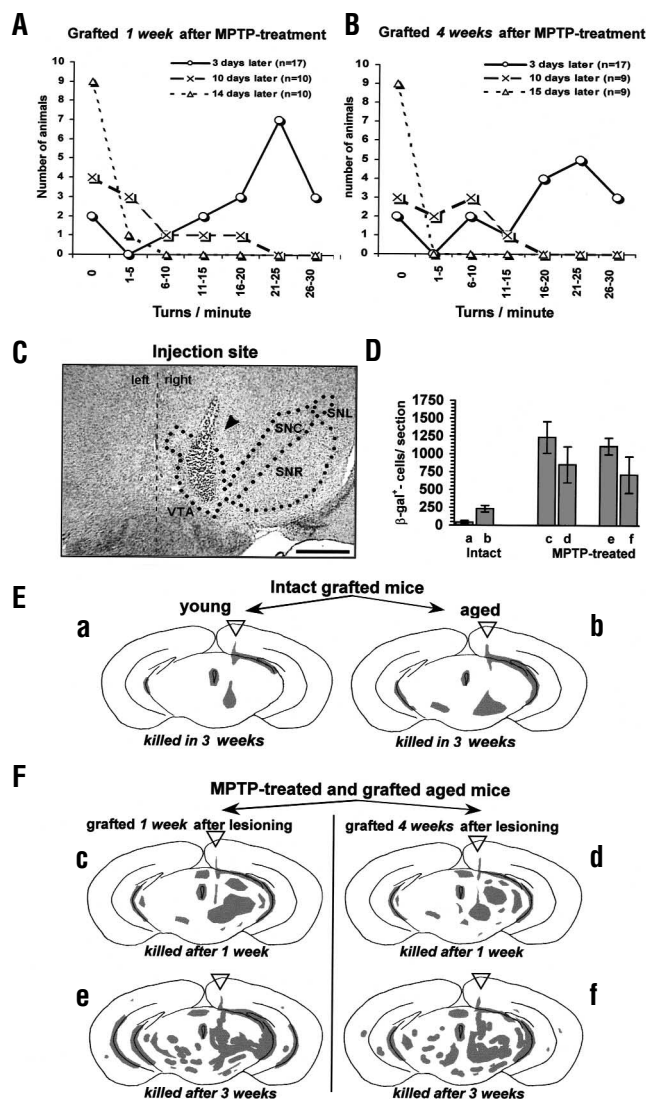
Expression of TH and DAT. Whereas the number of TH⁺ cells in sham-transplanted MPTP-lesioned mice remained very low bilaterally throughout the experimental period (and, in fact, the remaining lifespan of these aged animals), it increased substantially in the mesostriatal system after NSC transplantation (Figs 3, 4A). This re-expression of TH occurred gradually: one week after transplantation, TH activity was increased ($P < 0.01$) on the transplanted (right) but not the contralateral side (Fig. 4A, reflecting the immunocytochemical images in Fig. 3E, F). By three weeks post-transplant, the number of TH⁺ neurons in the mesostriatal nuclei became not only symmetrical (Fig. 4A, reflecting the immunocytochemical images in Fig. 3G, H), but actually approached—bilaterally—the values for an intact animal: compare the total number of TH⁺ cells in SN/VTA for both left and right hemispheres in Figure 4A with the number of TH⁺ cells in the intact SN/VTA as presented in Figure 1B. These numbers reflect and validate the histochemical impression conveyed in Figure 3 (compare Fig. 3G, H with Fig. 3A, B). The recovery of TH expression was slightly better in mice grafted one week after MPTP treatment (Fig. 4A) than in animals with delayed (four weeks) transplantation (Fig. 4B).

In addition to restored TH function in SN/VTA and striatum, an unusual TH expression pattern was noted above the mesostriatal nuclei (Fig. 3H). The time course of distribution of these ectopic cells (Fig. 4C, D) mirrored the gradual unilateral-to-bilateral changes seen in SN/VTA (Fig. 4A, B). Three weeks post-grafting, we found up to 400 ectopic TH⁺ cells/section in mice transplanted one week post-MPTP (Fig. 4C) and 150 ectopic cells in mice transplanted four weeks post-MPTP (Fig. 4D). Ectopic cells were never observed in sham-operated controls. Their derivation is assessed below and in Figure 5A–G.

We affirmed the graft-dependent reactivation of dopaminergic pathways by assaying the expression of an additional marker of renewed activity, the dopamine transporter (DAT) (Fig. 5H–J). One of the most reliable and specific markers for functional DA neurons²⁴, DAT expression was essentially absent in sham-grafted MPTP-lesioned mice (Fig. 5I), but in NSC-grafted MPTP-lesioned animals (Fig. 5J) it regained virtually the intensity observed in intact animals (Fig. 5H). A similar upregulation of DAT after grafting was found in the striatum but was weaker in the TH⁺ cells outside of the mesostriatal nuclei. (Note that sham-grafted animals (Fig. 5I) contained only punctuate residual DAT staining within their dysfunctional fibers, while, in normal and engrafted animals (Fig. 5H, J), DAT was present robustly in processes and cell bodies.)

The source of the TH⁺ neurons and fate of the donor-derived cells. Intriguingly, the reconstituted SN/VTA was composed primar-

Figure 2. (A,B) Analysis of D-amphetamine-evoked rotational behavior in MPTP-treated and grafted animals. Turning contralateral to the NSC-injected side was evaluated in mice injected systemically with amphetamine at 3, 10, and 14 days after grafting. The two graphs represent animals grafted (A) one or (B) four weeks after MPTP treatment. Absolute numbers of animals turning in a defined range of turns per minute are given. Although the mice showed robust turning during the first week after grafting, suggestive of DA asymmetry, this behavior disappeared progressively toward the end of the second week. This correlation of transient rotational behavior with unilaterally upregulated DA production and the presence of unilaterally implanted NSCs was subsequently supported histologically. (See Figures 2F, parts c,d; 3E, F; 4A, B). (C–F) Engraftment and distribution of β -gal⁺ NSCs in MPTP-treated and/or intact mouse brains. (C) Photomicrograph showing a detail from a hematoxylin-stained coronal section through the injection site area immediately after a unilateral stereotaxic deposit of NSCs (arrowhead, also in (E) and (F)) into the right SN/VTA. SNC, Substantia nigra pars compacta; SNR, substantia nigra pars reticularis; SNL, substantia nigra pars lateralis; VTA, ventral tegmental area. Bar, 750 μ m. (D) Histograms comparing quantitatively the distribution of the engrafted β -gal⁺ NSCs across both brain hemispheres. The letters below each histogram (a–f) refer to the camera lucida drawings in panels (E) and (F). In these panels, representative camera lucida drawings are presented showing the distribution (irrespective of cell densities) of β -gal⁺ NSCs in coronal brain sections, at the level of SN and VTA in (E) intact young (2-month-old) versus aged (20-month-old) mice, and in (F) MPTP-treated aged NSC-grafted mice killed after one or three weeks post-transplant. In contrast to the nonlesioned controls, aged MPTP-treated mice were characterized by extensive migration of grafted NSCs, whether grafting occurred one week (F, parts c, e) or four weeks (F, parts d, f) after MPTP lesioning. Whereas one week after grafting (F, parts c, d), donor cells were still mostly confined to the injected hemisphere and tended to cluster, by two weeks later they had dispersed widely across the midline and in a dorsoventral direction (F, parts e, f).



ily (~90%) of TH⁺ neurons that were of host origin (Figs 5A, 6), suggesting that they were “rescued” cells. Although ~10% of the TH⁺ cells in the mesencephalic nuclei were β -gal⁺ donor-derived (Fig. 5D), the majority of β -gal⁺ cells were actually located in the supranigral region (blocked area in Fig. 5A, magnified in Fig. 5B), where they helped give rise to the aforementioned population of “ectopic” TH neurons (Figs 4C, D and 5C), the composition of which was actually the inverse of the nuclei: 90% donor and, interestingly, ~10% host.

We further characterized the donor NSC-derived β -gal⁺ cells with antibodies recognizing antigens distinguishing the major neural cell types (Fig. 5). Approximately one-third of the grafted cells expressed markers of differentiation: ~70% were glia (mostly glial acidic fibrillary protein (GFAP⁺) and occasionally 2',3'-cyclic nucleotide 3'-phosphodiesterase (CNPase⁺)) (Fig. 5F, G) widely dispersed in mesencephalic gray and many fiber tracts; ~30% were NeuN⁺ (Fig. 5E), of which 5–10% expressed TH. As noted above, dual β -gal⁺/TH⁺ cells showed broad mesencephalic distribution but were a minority constituent of SN/VTA (Fig. 5A).

The remaining two-thirds of β -gal⁺ donor cells remained undifferentiated progenitors dispersed broadly throughout the mesencephalon. As detailed below, it is this subpopulation that might have been mediating the rescue of host TH⁺ neurons in the SN/VTA (Fig. 5A).

The expression of β -gal by TH⁺ donor-derived cells dorsal to SN/VTA (Fig. 5B) speaks against the simple misidentification of NSCs in SN/VTA as host cells because of *lacZ* downregulation. Nevertheless, this distinction between host- and donor-derived cells was confirmed by using an independent clone of NSCs expressing green fluorescent protein (GFP). Furthermore, we took advantage of the fact that host mice were female and the grafted NSCs were male. Because all female cells inactivate one of their X chromosomes, resulting invariably in the appearance of the Barr body in their nuclei²⁵, the origin of the reactivated TH⁺ cells could affirmatively be assigned as “host” by the presence of these female-specific chromatin structures, revealed by two independent methods: (i) the classic

nuclear histological stain and (ii) an immunostain with a Barr body-specific antibody²⁶ (Fig. 6).

The function of the ectopic TH⁺ cells remains unknown, but their presence was never reflected in any behavioral or histological aberrations or altered lifespan.

Rescued host neurons or new host neurons? Did nigral reconstitution by host TH⁺ cells represent the “rescue” of impaired neurons or the production of new ones? To help distinguish between these two possibilities, we administered sequential intraperitoneal injections of 5-bromo-2'-deoxyuridine (BrdU) (a marker of newly synthesized DNA) to all mice during the first postoperative week^{13,27} (Fig. 5K–M). Immunohistochemical detection of BrdU two weeks after the last BrdU pulse revealed that only nonneuronal (glial, endothelial, and meningeal) host cells (mostly around the site of NSC injection) had undergone mitosis (Fig. 5L, M). None of the TH⁺ cells incorporated BrdU (Fig. 5K), suggesting that neither MPTP nor NSC engraftment induced *de novo* neurogenesis in the host brain sufficient for repopulation of the mesostriatal system. Furthermore, the rapid (one to three weeks post-transplant) emergence of a wild type-like pattern of fully differentiated TH⁺ neurons in the SN/VTA with long-distance TH⁺ projections to the striatum (Fig. 3G, H) would seem to rule out complete re-establishment of this pathway from newly born host or donor precursors. Hence, we favor the interpretation that reconstitution of

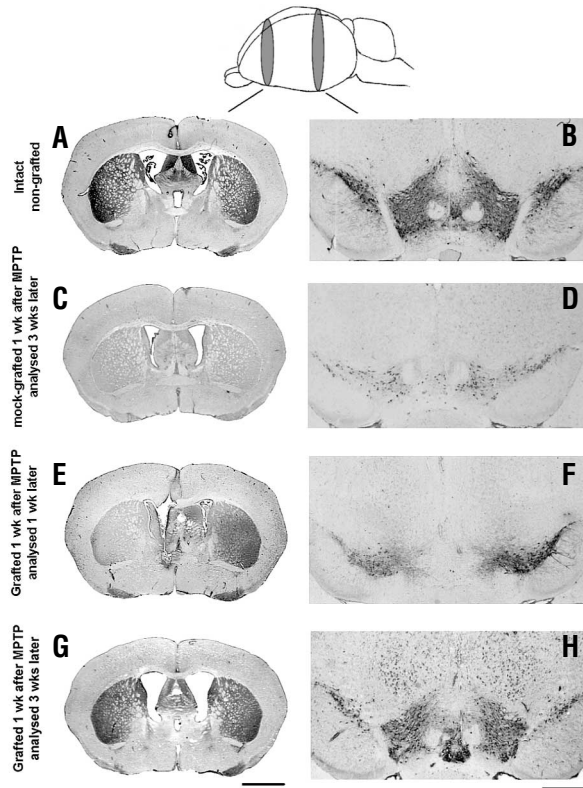


Figure 3. TH expression in mesencephalon and striatum of aged mice following MPTP lesioning and unilateral NSC engraftment into the SN/VTA area. Schematic on top indicates the levels of the analyzed transverse sections along the rostrocaudal axis of the mouse brain. Representative coronal sections through the striatum are presented in the left column (A, C, E, G) and through the SN/VTA area in the right column (B, D, F, H). (A, B) Immunodetection of TH (black cells) shows the normal distribution of DA-producing TH⁺ neurons in coronal sections in the intact SN/VTA (B) and their projections to the striatum (A). (C, D) Within one week, MPTP treatment caused extensive and permanent bilateral loss of TH immunoreactivity in both the the striatum (C) and the mesostriatal nuclei (D), which lasted for at least seven weeks (although was known to persist lifelong). Shown in this example, and matching the time point in (G, H), is the situation in a mock-grafted animal four weeks after MPTP treatment. (E, F) Unilateral (right side) stereotactic injection of NSCs into the nigra is associated, within one week after grafting, with substantial recovery of TH synthesis within the ipsilateral DA nuclei (F) and their ipsilateral striatal projections (E). (G, H) By three weeks post-transplant, however, the asymmetric distribution of TH expression disappeared, giving rise to TH immunoreactivity in the midbrain (H) and striatum (G) of both hemispheres that approached that of intact controls (A, B) and gave the appearance of mesostriatal restoration. Similar observations were made when NSCs were injected four weeks after MPTP treatment (not shown). Bars: 2 mm (left), 1 mm (right).

this dysfunctional system resulted from host cell rescue by implanted NSCs. Such reconstitution never occurred spontaneously throughout the lifespan of these aged mice.

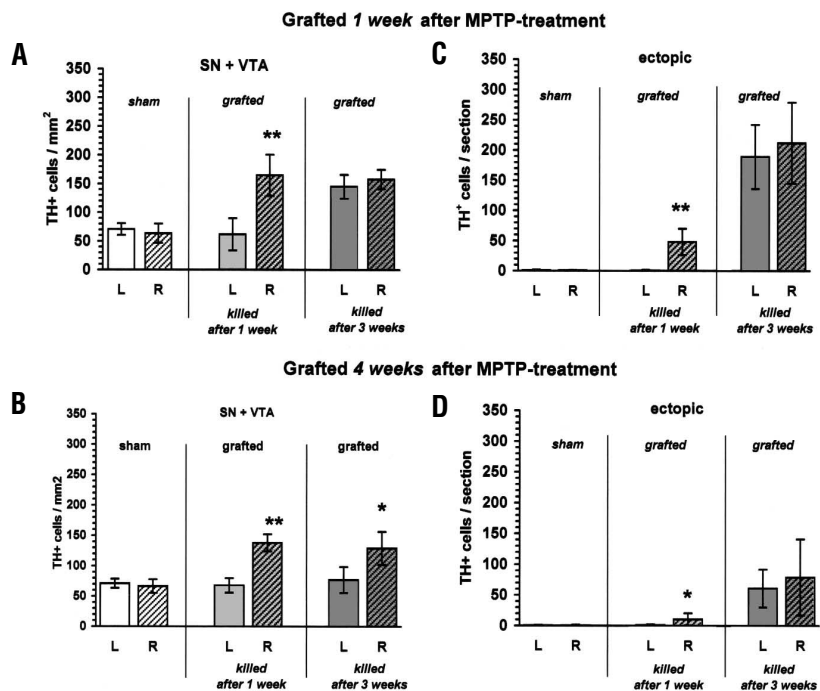
Possible mechanism underlying NSC-mediated rescue of DA neurons. Based on studies demonstrating the neuroprotective action of glial-cell-line-derived neurotrophic factor (GDNF) on DA neurons^{18,28,29}, we examined donor-derived cells *in vivo* for their expression of this neurotrophic factor. We know that undifferentiated NSCs

in vitro—but not their differentiated neuronal progeny—constitutively produce substantial amounts of various growth factors, including GDNF, without explicit genetic engineering (unpublished observations). Consistent with these data, we found a large subpopulation of small, undifferentiated donor-derived cells expressing GDNF *in vivo* (Fig. 7A, B, D). These GDNF-expressing cells, though sometimes in clusters in and around the injection site, were also extensively distributed bilaterally throughout the mesencephalon (Fig. 7B, D) (including in and around SN/VTA, magnified in Fig. 7D), periventricular zones, hippocampus, and neocortex. Differentiated β -gal⁺ cells expressing mature neuronal markers like TH (arrows in Fig. 7A, C) did not express GDNF (Fig. 7B). This factor likely represents one among a number of NSC-derived molecules impinging on DA neuronal function.

Discussion

In this study, we investigated the role of NSCs in a model of CNS maladies in which gradual but permanent functional impairment and oxidative stress are more prominent than cell death. Our prima-

Figure 4. Quantification of TH⁺ cells in nigral (A, B) and ectopic (C, D) brainstem regions of both hemispheres in mock-grafted (sham) and NSC-grafted MPTP-lesioned animals. Histological analyses were done one or three weeks after (A, C) acute (one week) and (B, D) delayed (four weeks) implantation of NSCs. Statistically significant differences (** $P < 0.001$; * $P < 0.01$) were calculated comparing left (L) and right (R) hemispheres in each animal within the same group to monitor the interhemispheric equilibration of TH levels in relation to the migration of the donor NSCs during the three-week period. Note that counts in SN/VTA (A, B) are given in cells/mm², while those in the ectopic areas (C, D) were evaluated in cells/section because of the very uneven cell distribution in these latter regions. While the reconstruction of the cellular pattern of TH expression in SN and VTA was similar whether grafting occurred one or four weeks after MPTP treatment (A, B) (although a slight interhemispheric difference in TH⁺ cell counts remained with delayed grafting in mice killed three weeks later), the number of ectopic TH⁺ cells (which is very low in intact and mock-grafted animals) was considerably increased after acute grafting. Delayed grafting yielded a decreased number of ectopic TH⁺ cells. Note that shams were examined at only three weeks.



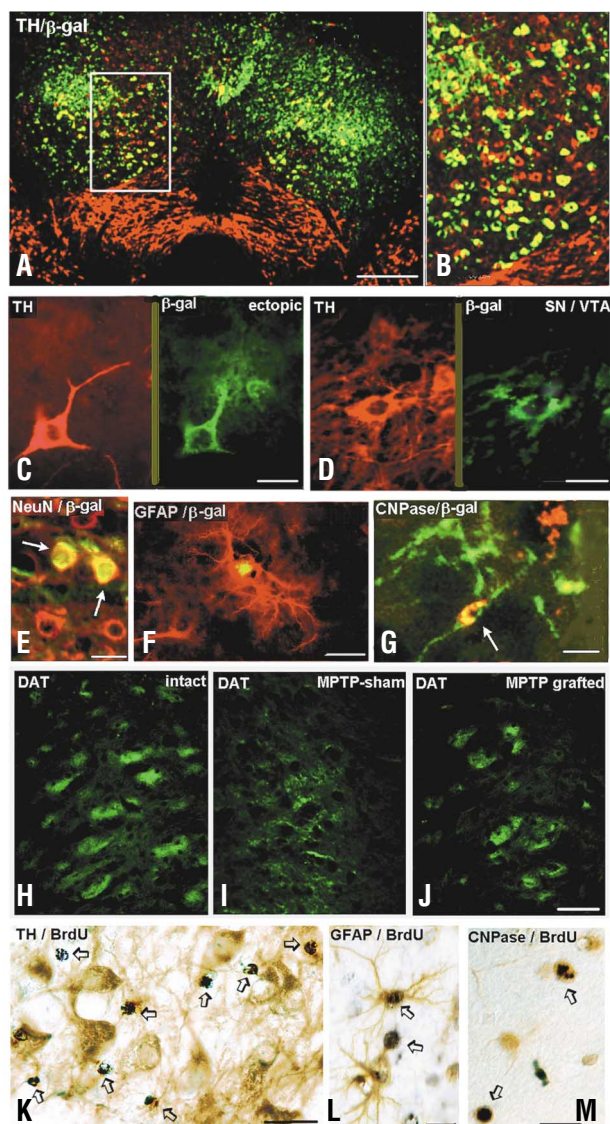


Figure 5. Immunohistochemical analyses of TH⁺, DAT⁺, and BrdU⁺ cells in MPTP-treated and grafted mouse brains. These photomicrographs were taken from immunostained brain sections from aged mice exposed to MPTP, transplanted one week later with NSCs, and killed after three weeks. The following combinations of markers were evaluated: TH (red) with β -gal (green) (A–D); NeuN (red) with β -gal (green) (E); GFAP (red) with β -gal (green) (F); CNPase (green) with β -gal (red) (G); as well as TH (brown) and BrdU (black) (K); GFAP (brown) with BrdU (black) (L); and CNPase (brown) with BrdU (black) (M). Anti-DAT-stained areas are revealed in green in the SN of intact brains (H), and in mock-grafted (I) and NSC-grafted (J) MPTP-treated brains. Three different fluorescence filters specific for Alexa Fluor 488 (green), Texas Red (red), and a double filter for both types of fluorochromes (yellow) were used to visualize specific antibody binding; (C), (D), and (H–J) are single-filter exposures; (A), (B), and (E–G) are double-filter exposures. (A, B) Low-power overview of the SN+VTA of both hemispheres, similar to the image in Figure 3H. The majority of TH⁺ cells (red) in (A) within the nigra are actually of host origin (~90%), with a much smaller proportion there being of donor derivation (green, ~10%). A representative close-up of such a donor-derived TH⁺ cell in the nigra can be seen in (D). Although a substantial proportion of NSCs did differentiate into TH⁺ neurons, many of these actually resided ectopically, dorsal to the SN (boxed area in (A), enlarged in (B); high-power view of an ectopic donor-derived (green) cell that was also TH⁺ (red) in (C)), where the ratio of donor to host cells was inverted: ~90% donor-derived compared with ~10% host-derived. Note the almost complete absence of a green β -gal-specific signal in the SN+VTA while, ectopically, many of the TH⁺ cells were double-labeled and thus NSC-derived, appearing yellow-orange in higher power under a red/green double filter in (B). (E–G) NSC-derived non-TH neurons (NeuN⁺; (E), arrow), astrocytes (GFAP⁺; (F)), and oligodendrocytes (CNPase⁺; (G), arrow) were also seen, both within the mesencephalic nuclei and dorsal to them. (H–J) The green DAT-specific signal in (J) suggests that the reconstituted mesencephalic nuclei in the NSC-grafted mice (as in panel (A) and Fig. 3H) were functional DA neurons comparable to those seen in intact nuclei (H) but not in MPTP-lesioned, sham-engrafted controls (I). This additionally suggests that the TH⁺ mesostriatal DA neurons affected by MPTP are, indeed, functionally impaired. (Note that sham-grafted animals (I) contain only punctate residual DAT staining within their dysfunctional fibers, while DAT staining in normal (H) and, similarly, in engrafted (J) animals was normally and robustly distributed both within processes and throughout their cell bodies.) (K–M) Any proliferative BrdU⁺ cells after MPTP insult and/or grafting (arrows) were confined to glial cells, while the TH⁺ neurons (K) were BrdU⁻. This finding suggested that the reappearance of TH⁺ host cells was not the result of neurogenesis but rather the recovery of extant host TH⁺ neurons—a conclusion reinforced in Figure 6. Bars: 90 μ m (A); 20 μ m (C–E); 30 μ m (F); 10 μ m (G); 20 μ m (H–J); 25 μ m (K); 10 μ m (L); 20 μ m (M).

ry conclusion is that transplanted NSCs may possess an inherent capacity to alter the recipient host environment such that the function of imperiled and/or dysfunctional endogenous neurons is reactivated or preserved.

Adjunctive to this conclusion are several other findings. First, aged brains can support the engraftment and extensive migration of NSCs. NSCs migrate even more readily in the aged brain (even without overt lesioning) than in the young adult intact brain, possibly in response to the spontaneous and progressive degeneration that characterizes aging neural tissue. In MPTP-treated aged animals, this migration was even more pronounced: implanted NSCs migrated readily across the midline and populated the mesencephalon as well as hippocampus and neocortex. Second, some NSCs can spontaneously differentiate into DA neurons in the DA-depleted brain. The NSCs were transplanted in an undifferentiated state, not pretreated with inductive factors or transduced with transgenes to direct their differentiation toward a dopaminergic lineage, as in other reports^{18,19,30,31}. The spontaneous differentiation by this subset of NSC progeny occurred in response to intrinsic host signals that are as yet unidentified but are probably related to the presence of impaired DA neurons and not to a “cellular void”, as observed elsewhere^{20,27,32}. Interestingly, none of the grafted NSCs in the intact young and aged brains spontaneously differentiated into TH⁺ neu-

rons, and no behavioral signs of DA excess were noted in these animals. The emergence of donor-derived DA neurons represents an example of an abnormal host environment “molding” the fate of exogenous NSCs. More important in this study, however, was evidence for a reciprocal dynamic: exogenous NSCs altering the recipient host CNS such that a more favorable milieu was established for the protection or rescue of imperiled host neurons, allowing the impaired mesostriatal DA system to become “reconstituted”.

The mechanism by which NSCs exert their influence—reflected in the tight linkage between donor-derived cells and the functional and histological reappearance of TH expression (Figs 2A, B and 3)—is likely to be complex. It is known that NSCs engineered *ex vivo* to deliver trophic factors like nerve growth factor (NGF)³³, GDNF¹⁸, and brain-derived neurotrophic factor (BDNF)²¹ can enhance neuronal survival and sprouting as effectively as when those factors are delivered by viral vectors^{28,34,35}. The graft-dependent neuroprotection observed in this study, however, occurred without the intercession of genetically engineered therapeutic transgenes to favor that process. Thus, NSCs seem to have an inherent capacity to preserve and reactivate cells through the natural expression of trophic and/or neuroprotective substances.

In most transplant studies, including the one reported here, a given engrafted region always contains a mixture of differentiated and undifferentiated NSC-derived cells. In our study, it was that latter pool (and possibly donor-derived astrocytes) that expressed GDNF. In earlier work²² we demonstrated that, during early CNS

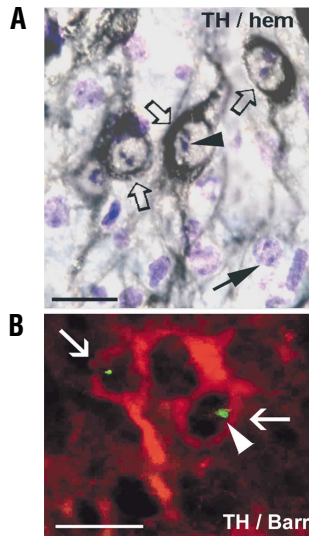


Figure 6. Rescued TH⁺ neurons in the SN/VTA of a transplanted female mouse are shown to be unambiguously of pre-existent host origin by demonstrating the presence of Barr bodies in their nuclei. The clone of NSCs used in all experiments (clone C17.2) was derived from a male, and most transplant recipients were female. Because all cells in a female must contain Barr bodies within their nuclei, cells of host (female) origin can be categorically distinguished from male cells by the presence of a Barr body. (A) TH⁺ neurons (black/brown anti-TH immunostain) (open arrows) counterstained with hematoxylin to show typical pairs of dense blue bodies in female nuclei—the nucleolus and the Barr body (arrowhead). Note the extensive well-developed TH⁺ processes in those female cells. Also note the presence of non-TH⁺ cells in the field (closed arrow) from this female brain that also contain Barr bodies. (B) The histological presence of Barr bodies in (A) is confirmed independently with a Barr body-specific antibody. Shown here are fluorescent double-immunostained nigral DA neurons immunoreactive to both TH-specific (red, cytoplasmic) (white arrows) and Barr body-specific (green, nuclear) (white arrowhead) antibodies. Bars, 20 μ m.

development, NSCs set aside pools of homeostasis-maintaining progenitors that intermingle with more mature clonal members and may provide “chaperones” for these more differentiated cells. Conceivably, a similar phenomenon allows for the rescue of host neurons even in old age. That the rescue is long-lived is suggested by the persistence of TH and DAT immunoreactivity within transplanted mice permitted to reach the end of a typical lifespan for this strain—in contrast to age-matched nongrafted and mock-grafted lesioned animals, in which this impairment remained unabated.

We do not exclude other types of stem/progenitor cells or primordial tissue from evoking—at least partially—a similar neuroprotective and rescue effect. The notion that, in transplantation experiments, NSCs not only accommodate to their hosts but may force their hosts to accommodate to them provides a reasonable explanation for previous perplexing observations^{13,14,36–38}. Occasionally, in the literature, recovery of function or anatomy was noted that could not plausibly be explained by the degree of differentiation or integration of donor tissue or the time frame over which such changes occurred. Such findings may now be explained if one invokes, as demonstrated here, the role of donor NSCs in promoting the spontaneous reorganization of host tissue even in the absence of differentiation toward cell replacement.

In summary, while NSCs have been used for neuronal replacement and gene therapy, these findings suggest a third mechanism by which therapeutic outcomes might be achieved: an inherent, constitutive capacity of NSCs (even in lieu of neuronal differentiation) to create host environments sufficiently rich in trophic and/or neuroprotective support to rescue imperiled host cells. The implications for CNS

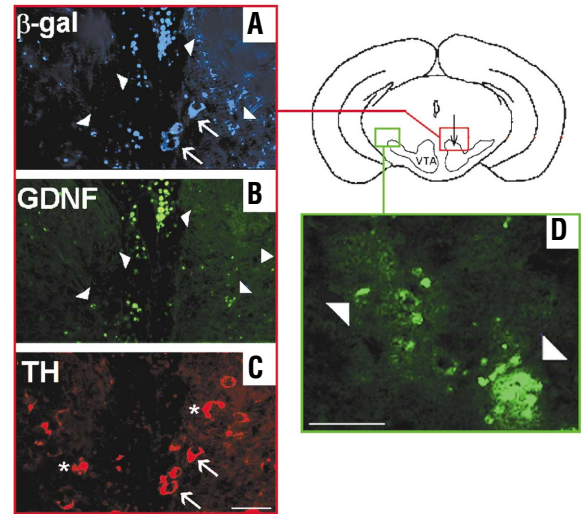


Figure 7. Grafted NSCs, in their undifferentiated state, intrinsically express GDNF in and adjacent to areas containing rescued host DA neurons. In sections from NSC-grafted brains of MPTP-treated mice, donor-derived cells in and around the rescued mesoatrial nuclei (e.g., red and green areas in schematic) were probed with immunohistochemistry for their expression of GDNF. Undifferentiated donor-derived (β -gal⁺) cells that were near the injection site or had migrated into parenchyma (A–C) as far as the contralateral hemisphere (D) expressed GDNF. (A–C) Triple immunolabeling revealing a subpopulation of small, undifferentiated donor-derived (β -gal⁺) (A), arrowheads) cells residing above the right VTA (red rectangle in schematic), together with two representative larger TH⁺ cells resembling differentiated donor-derived DA neurons (arrows). The small donor cells, negative for all the tested differentiation markers, were found to express substantial amounts of GDNF (B, arrowheads), a factor known to support regeneration of dysfunctional DA neurons. Anti-TH staining of the same region (C) showed the small donor cells to be negative for TH but revealed the presence of several host (β -gal⁺) mesoatrial neurons (asterisks). Donor-derived cells that had differentiated into TH⁺ cells in the ventral mesencephalon (arrows in C; compare to A) did not express GDNF (B). (D) Representative GDNF-expressing donor cells that had migrated to the contralateral supranigral region (green rectangle in schematic) are shown at higher power to demonstrate that protein's normal cytoplasmic location. VTA, ventral tegmental area; arrow in schematic indicates injection site. Bars, 80 μ m; bar in (C) applies also to (A) and (B).

repair are that one most likely needs to provide a variety of cell types—not just neurons, but also undifferentiated progenitors or glia to serve as “chaperones” (as seen in development)—to promote optimal recovery and a reconstructed organ. Dissecting the molecular determinants of this reciprocal intercellular signaling could also lead to new treatment approaches to progressive neurodegenerative diseases.

Experimental protocol

MPTP treatment. Aged (20 months, experimental) and young adult (2 months, control) C57BL/6J mice (principally female) were used (total = 104 animals). Animals were injected twice with MPTP, 30 mg/kg s.c. (Sigma, St. Louis, MO) at 0 and 5 h^{8,39} and transplanted one or four weeks later. Some were killed three weeks post-grafting (i.e., two months after the beginning of the study). Others were permitted to survive for an additional four months, typically the remainder of their lifespan (Supplementary Fig. 1 online).

NSCs and transplantation. Cells from NSC clone C17.2, which constitutively express *lacZ*, were grown and prepared as described^{1,2,4,20}. Some subclones were also engineered by retrovirus-mediated gene transfer to express GFP.

Mice were anesthetized (75 mg/kg of sodium pentobarbital), the skull was disinfected, and a 1-cm-long parasagittal incision of skin and subcutaneous

tissue was performed above the right tegmental area. Using a stereotactic frame, through a 0.9-mm-diameter hole in the skull (2.6 mm anterior to lambda; 1.5 mm lateral to the sagittal suture⁴⁰), a 2 μ l volume (4–5 \times 10⁴ cells/ μ l) of NSCs in Hank's balanced salt solution (HBSS) was injected (over 2 min) unilaterally into the right SN/VTA area (depth 4 mm). Mock-grafted controls received the same volume of HBSS. The skin was re-approximated with cyanoacrylate glue.

D-Amphetamine rotation test. D-Amphetamine sulfate (2% in saline, 5 mg/kg/dose i.p.) was administered to mice at 3, 10, and 14 days after transplantation. Rotational scores were recorded in absolute numbers over 30 min. Shams and intact mice were injected in parallel as controls.

BrdU injections. Mice received injections of BrdU (50 mg/kg/dose i.p.) on days 2, 4, and 6 after transplantation or MPTP treatment. BrdU⁺ cells were detected immunohistochemically three weeks after transplantation as described¹⁴. The schedule, though suboptimal for labeling a maximum of proliferating cells (assuming a cell cycle length of 12–14 h), minimized the number of injections and possible BrdU-related toxicity^{41,42}.

Histology. Brains were embedded in polyester wax as described¹³ and 20 μ m serial coronal sections were collected.

Immunohistochemistry. Dewaxed and rehydrated sections were blocked, and β -gal was detected with a mouse monoclonal antibody ((mAb) 1:300; Promega, Madison, WI) or a rabbit polyclonal antibody ((pAb) 1:100; ICN/Cappel, Costa Mesa, CA). Anti-BrdU immunostains were conducted by standard techniques¹⁴ with a rat mAb (1:75; Serotec, Raleigh, NC), followed by a cell type-specific immunostain. Cell type-specific antigens were detected with the following antibodies: NeuN with a mouse mAb (1:100; gift from R. Mullen); TH with a mouse mAb (1:5,000; Sigma); GDNF with either a mouse mAb (1:200; Chemicon, Temecula, CA) or a goat pAb (1:100; Research Diagnostics, Flanders, NJ); anti-DAT with a rabbit pAb (1:50; Chemicon); GFAP (defining astrocytes) with a rabbit pAb (1:500; Sigma); CNPase (defining oligodendrocytes) with a mouse mAb (1:250; Promega). Barr bodies were detected by antiserum 3286 (1:300; gift from T. Yang and W. Brooks). All dilutions occurred in the blocking solution, and incubations occurred overnight at 4°C. Primary antibodies were detected with biotinylated antibodies and 3,3'-diaminobenzidine tetrahydrochloride (DAB) according to the Vectastain kit protocol (Vector Laboratories, Burlingame, CA). For simultaneous detection of β -gal, BrdU, or Barr bodies with cell type-specific markers, double and triple immunostaining using epifluorescence was carried out with secondary antibodies coupled to fluorochromes Alexa Fluor 488 and Alexa Fluor 594 (Molecular Probes, Eugene, OR) and Texas Red (Vector) (used according to the manufacturer's protocol).

Quantitation. Cell counts were obtained from three sections per animal taken from the rostral (level 335), medial (level 343), and caudal (level 360) regions of the area serially cut between levels 330 and 361 (ref. 40) containing the major portions of SN and VTA, the borders of which were delineated by TH immunostains in intact brains. From these, camera lucida overlays were prepared and superimposed on sections from corresponding brain regions and oriented according to structures such as hippocampus and ventricles. Cell counts in SN/VTA were evaluated using a reticle eyepiece (magnifying 40 \times 10) and expressed either in cells/mm² (e.g., Figs 1, 4A, B) or cells/section when totaling donor (β -gal⁺) and ectopic TH⁺ cells (e.g., Figs 2D and 4C, D). The evaluations were done "blindly" and the results were presented as means \pm s.e.m. Cell counts per unit area were corrected for split cell error. ANOVA with post hoc Newman-Keuls test was used to analyze differences in cell numbers between groups. Paired *t*-test was used to compare interhemispheric differences in DA neuron counts ($P < 0.001$ and $P < 0.01$). As a confirmation of the sensitivity of the system described above for assessing even subtle changes in cell numbers, the following preliminary calculations were done: in an intact SN/VTA, there are on average 480 neurons/mm², 48% of which (230 cells) are TH⁺. A reduction of TH positivity by 61% corresponds to \sim 140 DA neurons/mm². Neuronal cell loss, as assessed by counts of NeuN⁺ cells, would be reflected as a 29% reduction, that is, from 480 to 340 cells/mm², readily detectable by this technique. Such total neuron losses were not detected, although losses in TH immunoreactivity within the same cell population could sensitively be assayed.

Note: Supplementary information is available on the Nature Biotechnology website.

Acknowledgments

We thank Tom Yang and Wesley Brooks for their gift of the Barr body-specific immune serum and Mahesh Lachyankar in the Snyder laboratory for sharing unpublished data. We also thank Yvonne Bruderer and Markus Rimann for technical assistance, Kathrin Mannigel for maintenance of the animal colony, and Donald E. Mitchell, Olga Kukal, and Tom Allen for input. This work was supported in part by grants from the Swiss National Research Foundation to M.S., the Michael J. Fox/Parkinson Action Network to V.O., the International Institute for Research in Paraplegia, Zurich, to V.O. and E.Y.S., National Institutes of Neurological Diseases and Stroke, the A-T Children's Project, March of Dimes, Project ALS and the International Organization for Glutamic Acidemia to E.Y.S.

Competing interests statement

The authors declare that they have no competing financial interests.

Received 10 April 2002; accepted 9 August 2002

1. Aboody, K.S. *et al.* Neural stem cells display extensive tropism for pathology in adult brain: evidence from intracranial tumors. *Proc. Natl. Acad. Sci. USA* **97**, 12846–12851 (2000).
2. Yandava, B.D., Billingham, L.L. & Snyder, E.Y. "Global" cell replacement is feasible via neural stem cell transplantation: evidence from the dysmyelinated shiverer mouse brain. *Proc. Natl. Acad. Sci. USA* **96**, 7029–7034 (1999).
3. Bjorklund, A. & Lindvall, O. Cell replacement therapies for central nervous system disorders. *Nat. Neurosci.* **3**, 537–544 (2000).
4. Snyder, E.Y., Yoon, C., Flax, J.D., & Macklis, J.D. Multipotent neural precursors can differentiate toward replacement of neurons undergoing targeted apoptotic degeneration in adult mouse neocortex. *Proc. Natl. Acad. Sci. U.S.A.* **94**, 11663–11668 (1997).
5. Ourednik, V., Ourednik, J., Park, K.I. & Snyder, E.Y. Neural stem cells—a versatile tool for cell replacement and gene therapy in the central nervous system. *Clin. Genet.* **56**, 267–278 (1999).
6. Snyder, E.Y., Taylor, R.M. & Wolfe, J.H. Neural progenitor cell engraftment corrects lysosomal storage throughout the MPS VII mouse brain. *Nature* **374**, 367–370 (1995).
7. Grunblatt, E., Mandel, S., Maor, G. & Youdim, M.B.H. Gene expression analysis in *N*-methyl-4-phenyl-1,2,3,6-tetrahydropyridine mice model of Parkinson's disease using cDNA microarray: effect of *R*-apomorphine. *J. Neurochem.* **78**, 1–12 (2001).
8. Sonsalla, P.K. & Heikkila, R.E. The influence of dose and dosing interval on MPTP-induced dopaminergic neurotoxicity in mice. *Eur. J. Pharmacol.* **129**, 339–345 (1986).
9. Heikkila, R.E., Hess, A. & Duvoisin, R.C. Dopaminergic neurotoxicity of 1-methyl-4-phenyl-1,2,5,6-tetrahydropyridine in mice. *Science* **224**, 1451–1453 (1984).
10. Gerlach, M. & Riederer, P. Animal models of Parkinson's disease: an empirical comparison with the phenomenology of the disease in man. *J. Neural Transm.* **103**, 987–1041 (1996).
11. Przedborski, S. & Jackson-Lewis, V. Mechanisms of MPTP toxicity. *Mov. Disord.* **13** (Suppl. 1), 35–38 (1998).
12. Hamre, K., Tharp, R., Poon, K., Xiong, X. & Smeyne, R.J. Differential strain susceptibility following 1-methyl-4-phenyl-1,2,3,6-tetrahydropyridine (MPTP) administration acts in an autosomal dominant fashion: quantitative analysis in seven strains of *Mus musculus*. *Brain Res.* **828**, 91–103 (1999).
13. Ourednik, J., Ourednik, W. & Van der Loos, H. Do foetal neural grafts induce repair by the injured juvenile neocortex? *Neuroreport* **5**, 133–136 (1993).
14. Ourednik, J., Ourednik, W. & Mitchell, D.E. Remodeling of lesioned kitten visual cortex after xenotransplantation of fetal mouse neopallium. *J. Comp. Neurol.* **395**, 91–111 (1998).
15. Desai, V.G., Feuers, R.J., Hart, R.W. & Ali, S.F. MPP(+)-induced neurotoxicity in mouse is age-dependent: evidenced by the selective inhibition of complexes of electron transport. *Brain Res.* **715**, 1–8 (1996).
16. Mandavilli, B.S., Ali, S.F. & Van Houten, B. DNA damage in brain mitochondria caused by aging and MPTP treatment. *Brain Res.* **885**, 45–52 (2000).
17. Heikkila, R.E., Sieber, B.A., Manzino, L. & Sonsalla, P.K. Some features of the nigrostriatal dopaminergic neurotoxin 1-methyl-4-phenyl-1,2,3,6-tetrahydropyridine (MPTP) in the mouse. *Mol. Chem. Neuropathol.* **10**, 171–183 (1989).
18. Akerud, P., Canals, J.M., Snyder, E.Y. & Arenas, E. Neuroprotection through delivery of glial cell line-derived neurotrophic factor by neural stem cells in a mouse model of Parkinson's disease. *J. Neurosci.* **21**, 8108–8118 (2001).
19. Wagner, J. *et al.* Induction of a midbrain dopaminergic phenotype in Nurr1-overexpressing neural stem cells by type 1 astrocytes. *Nat. Biotechnol.* **17**, 653–659 (1999).
20. Rosario, C.M. *et al.* Differentiation of engrafted multipotent neural progenitors towards replacement of missing granule neurons in meander tail cerebellum may help determine the locus of mutant gene action. *Development* **124**, 4213–4224 (1997).
21. Rubio, F.J. *et al.* BDNF gene transfer to the mammalian brain using CNS-derived neural precursors. *Gene Ther.* **6**, 1851–1866 (1999).
22. Ourednik, V. *et al.* Segregation of human neural stem cells in the developing primate forebrain. *Science* **293**, 1820–1824 (2001).
23. Ungerstedt, U. & Arbuthnott, G.W. Quantitative recording of rotational behavior in rats after 6-hydroxy-dopamine lesions of the nigrostriatal dopamine system. *Brain*

- Res. **24**, 485–493 (1970).
24. Kuhar, M.J. Recent biochemical studies of the dopamine transporter—a CNS drug target. *Life Sci.* **62**, 1573–1575 (1998).
 25. Barr, M.L. & Bertram, E.G. A morphological distinction between neurones of the male and female, and the behaviour of the nucleolar satellite during accelerated nucleoprotein synthesis. *Nature* **163**, 676–677 (1949).
 26. Hong, B., Reeves, P., Panning, B., Swanson, M.S. & Yang, T.P. Identification of an autoimmune serum containing antibodies against the Barr body. *Proc. Nat. Acad. Sci. USA* **98**, 8703–8708 (2001).
 27. Magavi, S.S., Leavitt, B.R. & Macklis, J.D. Induction of neurogenesis in the neocortex of adult mice. *Nature* **405**, 951–955 (2000).
 28. Kordower, J.H. *et al.* Neurodegeneration prevented by lentiviral vector delivery of GDNF in primate models of Parkinson's disease. *Science* **290**, 767–773 (2000).
 29. Choi-Lundberg, D.L. *et al.* Dopaminergic neurons protected from degeneration by GDNF gene therapy. *Science* **275**, 838–841 (1997).
 30. Studer, L., Tabar, V. & McKay, R.D. Transplantation of expanded mesencephalic precursors leads to recovery in parkinsonian rats. *Nat. Neurosci.* **1**, 290–295 (1998).
 31. Storch, A. *et al.* Long-term proliferation and dopaminergic differentiation of human mesencephalic neural precursor cells. *Exp. Neurol.* **170**, 317–325 (2001).
 32. Bjorklund, L.M. *et al.* Embryonic stem cells develop into functional dopaminergic neurons after transplantation in a Parkinson rat model. *Proc. Natl. Acad. Sci. USA* **99**, 2344–2349 (2002).
 33. Martinez-Serrano, A. *et al.* CNS-derived neural progenitor cells for gene transfer of nerve growth factor to the adult rat brain: complete rescue of axotomized cholinergic neurons after transplantation into the septum. *J. Neurosci.* **15**, 5668–5680 (1995).
 34. Bjorklund, A. *et al.* Towards a neuroprotective gene therapy for Parkinson's disease: use of adenovirus, AAV and lentivirus vectors for gene transfer of GDNF to the nigrostriatal system in the rat Parkinson model(1). *Brain Res.* **886**, 82–98 (2000).
 35. Lowenstein, P.R. & Castro, M.G. Genetic engineering within the adult brain: implications for molecular approaches to behavioral neuroscience. *Physiol. Behav.* **73**, 833–839 (2001).
 36. Ourednik, W. & Ourednik, J. Newly formed host cells in a grafted juvenile neocortex express neurone-specific marker proteins. *Neuroreport* **5**, 1073–1076 (1994).
 37. Hodges, H. *et al.* Conditionally immortal neuroepithelial stem cell grafts reverse age-associated memory impairments in rats. *Neuroscience* **101**, 945–955 (2000).
 38. Veizovic, T., Beech, J.S., Stroemer, R.P., Watson, W.P. & Hodges, H. Resolution of stroke deficits following contralateral grafts of conditionally immortal neuroepithelial stem cells. *Stroke* **32**, 1012–1019 (2001).
 39. Date, I., Notter, M.F., Felten, S.Y. & Felten, D.L. MPTP-treated young mice but not aging mice show partial recovery of the nigrostriatal dopaminergic system by stereotaxic injection of acidic fibroblast growth factor (aFGF). *Brain Res.* **526**, 156–160 (1990).
 40. Sidman, R.L., Angevine, J.B., Jr. & Taber-Pierce, E. *Atlas of the Mouse Brain and Spinal Cord* (Harvard University Press, Cambridge, MA, 1971).
 41. Webster, W., Shimada, M. & Langman, J. Effect of fluorodeoxyuridine, colcemid, and bromodeoxyuridine on developing neocortex of the mouse. *Am. J. Anat.* **137**, 67–85 (1973).
 42. Cai, L., Hayes, N.L. & Nowakowski, R.S. Local homogeneity of cell cycle length in developing mouse cortex. *J. Neurosci.* **17**, 2079–2087 (1997).